PHOTOMASK

BACUS—The international technical group of SPIE dedicated to the advancement of photomask technology.

BACUS NEWS

MAY 2015
VOLUME 31, ISSUE 5

3rd Place Winner for Best Poster - SPIE Photomask Technology 2014

Recent results from EUVL patterned mask inspection using Projection Electron Microscope system

Ryoichi Hirano, Susumu Iida, Tsuyoshi Amano, Tsuneo Terasawa, and Hidehiro Watanabe, EUVL Infrastructure Development Center, Inc. 16-1 Onogawa, Tsukuba-shi, Ibaraki-ken, 305-8569, Japan.

Masahiro Hatakeyama, Takeshi Murakami, Shoji Yoshikawa, and Kenji Terao, EBARA CORPORATION, 4-2-1, Honfujisawa, Fujisawa-shi 251-8502, Japan

ABSTRACT

The recent status of a newly developed PEM pattern inspection system for hp 16 nm node defect detection is presented. A die-to-die defect detection sensitivity of the developing system is also investigated. A programmed defect mask was used for demonstrating the performance of the system. Defect images were obtained as difference images by comparing the PEM images "with defects" to the PEM images "without-defects". This image-processing system was also developed for die-to-die inspection. Captured images of extrusion and intrusion defects in hp 64 nm L/S pattern were used for detection. 12 nm sized intrusion defect, that was smaller than our target size for hp 16 nm defect detection requirement, was identified without false defects. To improve the performance of hp 16 nm patterned mask inspection for hp 11 nm EUVL patterned mask inspection, defect detection signal characteristics, which depend on hp 64 nm pattern image intensity deviation on EUVL mask, was studied.

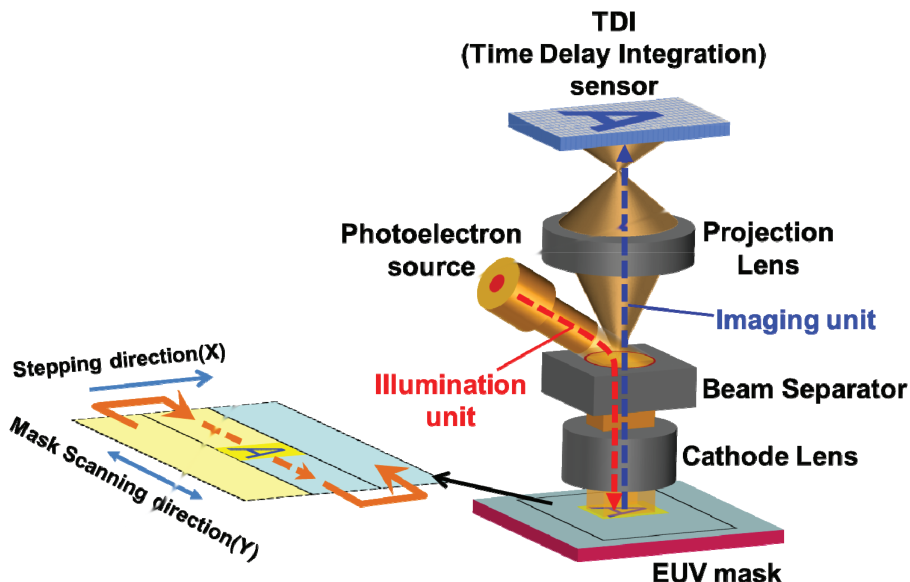

Figure 1. Schematic diagram of a PEM system.

TAKE A LOOK INSIDE:

INDUSTRY BRIEFS
—see page 9

CALENDAR
For a list of meetings
—see page 10

SPIE.

9235-47

EDITORIAL

Why doesn't the sun shine upside down anymore?

Michael T. Postek, Semiconductor and Dimensional Metrology Division, National Institute of Standards and Technology, Gaithersburg, MD 20855

It is high noon, the sun is directly overhead and the view is looking downward from that perspective. Yet the shadows from the topography of the landscape still fall to the northwest and the edges are greatly enhanced and highlighted. I step forward and nearly slip off a cliff since the actual location of the edge was obscured by those highlights. Where is the edge? I must be careful and accurately place my feet. But, was it always that way? There once was a time when the sun shone from below and the world was once viewed upside down, yet the view and highlights would have been similar. The reasons for the illumination geometry have been lost in antiquity, but now, is it really the right side up? Can we say for sure? We have little first-hand experience in the microscopic world, and as such proper interpretations of any microscopic images are crucial to many industrial applications. Just as crucial as seeing or detecting the accurate location of the cliff edge or in an application such as critical dimension metrology – that is, unless you want to fall, or fail.

How hard can microscopy be? A sample is grabbed and mounted, a button is pushed here and there, a vacuum is pulled and an image shows up over there after some electrons or ions hit here, and signal is generated there, and there, and there. Reams of data are taken. What should we do? What should we do? Clearly, the answer to the question is to attend the upcoming SPIE/Scanning Microscopies meeting and learn more about the scanned beam and probe instruments being used every day in a variety of research and industrial applications. Historically, the Scanning Microscopies conference has been largely associated with the "how's" and "why's" and so its intent has been more technique and application oriented. Overall the Scanning Microscopies series of meetings have a long history and has strongly contributed to the success of these various forms of microscopy.

The Scanning Microscopies meeting also fosters microscopy education through its in science, technology, engineering and math (STEM) sessions. For the fourth year, the Scanning Microscopies Conference will hold a special session for STEM Educators. In the previous sessions, STEM educators from across the country have presented their successes in utilizing microscopy in course curriculums. Sufficient time has now passed and now encouraging data is beginning to come to light demonstrating that microscopy, even introduced into elementary education, fosters inquiry. Those students having that opportunity have been shown to have vastly improved test scores. Fully functional tabletop scanning electron microscopes and atomic force microscopes have been brought into the conference room for attendees use. This year, Ben Dubin-Thaler who is the originator of the BioBus (http://biobus.org/) will bring the "rolling laboratory" to the site and will speak in the STEM session.

The SPIE 2015 SPIE Scanning Microscopies Conference is pleased to be co-locating again with the Photomask Technologies Conference, in Monterey. The Scanning Co-chairs are Dale Newbury, Frank Platek, Tim Maugel and Michael T. Postek. This is the second year of this highly successful co-location and another banner year is anticipated. This conference is re-building and co-locating this meeting with the Photomask Technology Conference has provided a strong synergy between the technologies since so many of the Photomask manufacturers and researchers routinely utilize the various forms of scanned microscopies in research and manufacturing. Photomask Technology attendees are more than welcome to participate in any of the Scanning Microscopies sessions and are encouraged submit papers to the conference. Student participation is highly encouraged.

N • E • W • S

BACUS News is published monthly by SPIE for BACUS, the international technical group of SPIE dedicated to the advancement of photomask technology.

Managing Editor/Graphics Linda DeLano
Advertising Lara Miles
BACUS Technical Group Manager Pat Wight

■ 2015 BACUS Steering Committee ■

President
Paul W. Ackmann, *GLOBALFOUNDRIES Inc.*

Vice-President
Jim N. Wiley, *ASML US, Inc.*

Secretary
Larry S. Zurbrick, *Keysight Technologies, Inc.*

Newsletter Editor
Artur Balasinski, *Cypress Semiconductor Corp.*

2015 Annual Photomask Conference Chairs
Naoya Hayashi, *Dai Nippon Printing Co., Ltd.*
Bryan S. Kasprowicz, *Photronics, Inc.*

International Chair
Uwe F. W. Behringer, *UBC Microelectronics*

Education Chair
Artur Balasinski, *Cypress Semiconductor Corp.*

Members at Large
Frank E. Abboud, *Intel Corp.*
Paul C. Allen, *Toppan Photomasks, Inc.*
Michael D. Archuletta, *RAVE LLC*
Peter D. Buck, *Mentor Graphics Corp.*
Brian Cha, *Samsung*
Thomas B. Faure, *IBM Corp.*
Brian J. Grenon, *Grenon Consulting*
Jon Haines, *Micron Technology Inc.*
Mark T. Jee, *HOYA Corp, USA*
Patrick M. Martin, *Applied Materials, Inc.*
M. Warren Montgomery, SUNY, *The College of Nanoscale Science and Engineering*
Wilbert Odisho, *KLA-Tencor Corp.*
Jan Hendrik Peters, *Carl Zeiss SMS GmbH*
Michael T. Postek, *National Institute of Standards and Technology*
Abbas Rastegar, *SEMATECH North*
Emmanuel Rausa, *CYMER LLC.*
Douglas J. Resnick, *Canon Nanotechnologies, Inc.*
Thomas Struck, *Infineon Technologies AG*
Bala Thumma, *Synopsys, Inc.*
Jacek K. Tyminski, *Nikon Research Corp. of America (NRCA)*
Michael Watt, *Shin-Etsu MicroSi, Inc.*

SPIE.

P.O. Box 10, Bellingham, WA 98227-0010 USA
Tel: +1 360 676 3290
Fax: +1 360 647 1445
www.SPIE.org
help@spie.org

©2015

All rights reserved.

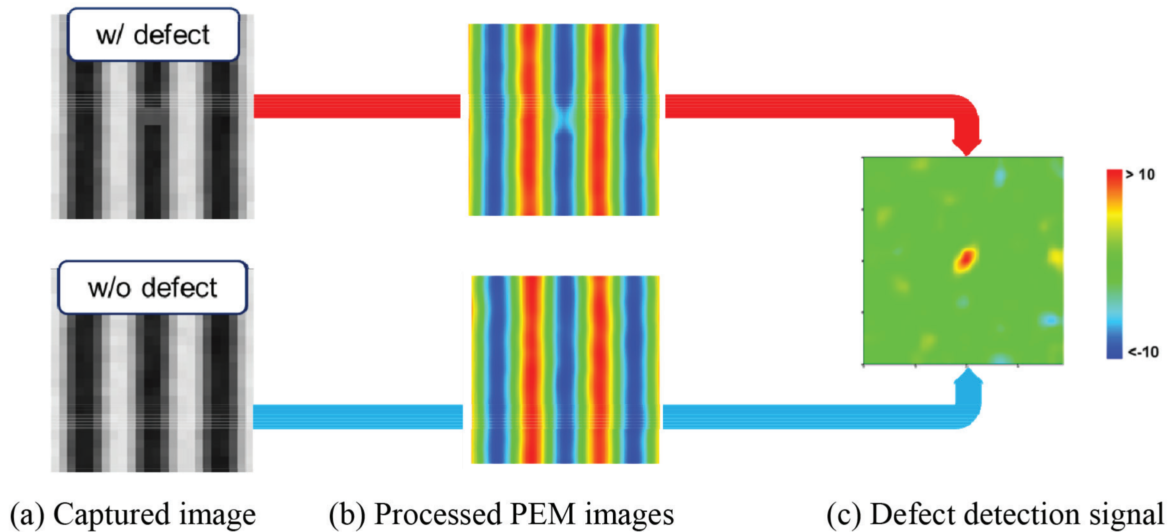

Figure 2. Schematics of defect detection sequence.

1. Introduction

Extreme Ultraviolet Lithography (EUVL) stands as the foremost next-generation lithographic technology after the ArF immersion lithography has reached its limit to deliver smaller features. EUVL mask pattern defect detection is one of the major issues to realize device fabrication with EUV lithography.[1-6] As prescribed by the ITRS 2013 Edition, and based on defect printability simulation, the sensitivity requirement for EUV patterned mask inspection system at sub-16 nm nodes is investigated.[14,15] We have designed a novel Projection Electron Microscopy (PEM) system, which has proven to be quite promising for hp 1Xnm node mask inspection.[7-12] Currently, the PEM optics is integrated with a pattern inspection system for the defect detection sensitivity evaluation. Model EBEYE-V30 ("Model EBEYE" is an EBARA's model code) inspection system has a high resolution and high-throughput electron optics. To study the PEM optics system, its potentials for making to the 1X nm node had been addressed by evaluating its die-to-die defect detection sensitivity. A programmed defect mask was used for demonstrating the performance of the system.[13] Defect images were obtained as difference images by comparing the PEM images "with-defects" to the PEM images "without-defects". The image-processing system was also developed for a die-todie inspection. A targeted inspection throughput of 19-hour inspection per mask with 16 nm pixel size for hp 16 nm node defect detection could be attained.[16] We reported on the recent results of EUVL patterned mask inspection using the developing PEM system. And now we discuss the systems extendibility to sub-16-nm node defect detection with system improvements in the PEM optics and defect detection signal processing.

2. Design Concept and Current Status of the Developing PEM System

Figure 1 shows a schematic illustration of the PEM system. For the illumination optics, an electron beam is generated from a photoelectron source, and then the beam is deflected by a beam separator. Mask surface is then illuminated through a cathode lens. The design of the imaging optics consists of a cathode lens and a projection lens. Electron image generated at the mask is then focused onto a time-delay integration (TDI) sensor. In scanning the full area during a mask inspection, the mask is scanned in Y direction where a swath image of TDI sensor is captured using its TDI mode option and then step in the X direction. Thus repeating the step and scan movement, the full mask area can be inspected. By its design, the illuminated area is sufficiently large to cover the entire sensor area. The system shows the detection capability for defects in hp 64 nm in the EUVL mask. And this system enables a 19-hour long inspection time resulting in a throughput determined by a data processing rate of 600MPPS (Mega Pixel Per Second) and a pixel size of 16 nm. And that was then confirmed by measuring an actual mask scanning time. Development of defect detection performance for 16 nm HVM, and studies on hp 11 nm Patterned mask Inspection (PI) technologies are currently in progress.[16]

3. Die-to-Die Inspection Experiment

Figure 2 shows the schematics of defect detection sequence using the signal processing. Electron image generated at the mask is focused onto a time-delay integration sensor.

The capturing image of a L/S pattern on a sample EUVL mask, with and without pin dot defects are loaded onto an image-processing system (Fig. 2 (a)). After enhancing the defect signal, that was run through the image-processing system (Fig. 2 (b)), processing image of "without-defect" was subtracted from the processing image of "with-defect" (Fig. 2 (c)). The defect was then detected by the defect detection signal.

3.1 Defect detection sensitivity evaluation by capturing image of a programmed pattern defect

Previously, an example of a die-to-die defect inspection result by applying the developed defect detection algorithm was presented.[13] Defect detection sensitivity evaluation was executed with 16 nm size intrusion defects as the targeted defect size for 16 nm node defect detection. And the defect detection sensitivity was carried out for 28 nm sized extrusion defect; the defect could then be identified, although several false defects were also encountered. There still is a need for further improvement to satisfy the hp 16 nm HVM requirements.16 For the estimation of defect detection requirements for hp 11 nm node devices, reference14

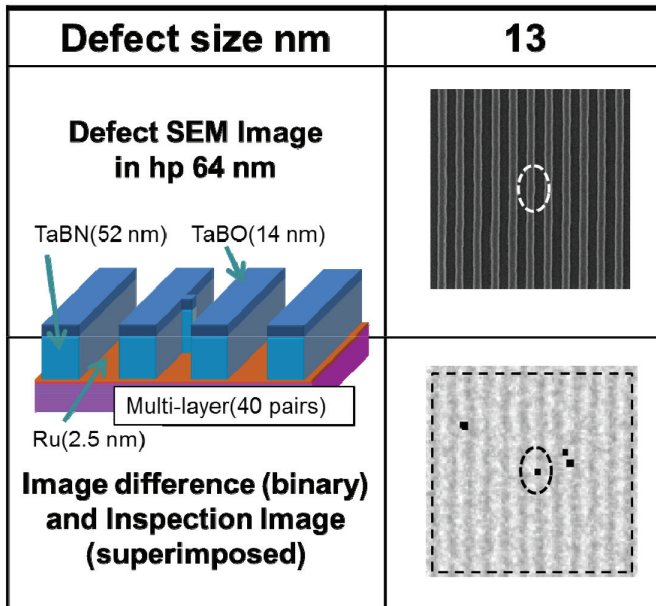

Figure 3. Defect detection sensitivity evaluation result for extrusion defect.

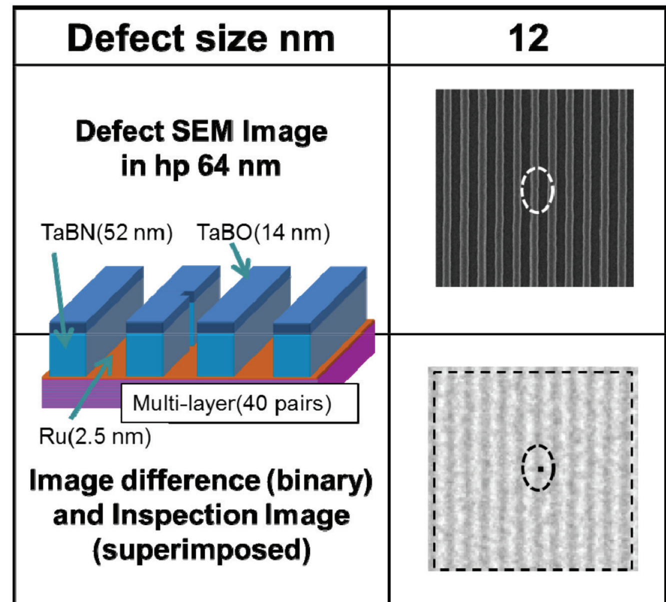

Figure 4. Defect detection sensitivity evaluation result for intrusion defect.

is made to the ITRS 2013 Edition that specifies the requirement of 1X nm EUV mask. In order to address pattern size for hp 11 nm on wafer, we focused on a minimum primary feature size of 44 nm on mask. So, it is established that smaller than 13 nm size defect detection would be necessary in order to realize the hp 11 nm node pattern fabrications. In order to predict the defect detection, we also employed a printability simulator. From the simulation, it is learned that more than 13 nm extrusion defect, or more than 20 nm intrusion defect, can cause more than 10% Critical Dimension (CD) error for hp 11 nm EUV lithography.[15]

These values have roughly met the specifications as prescribed by the ITRS 2013 Edition. So for hp 11 nm node EUV mask pattern defect detection, we targeted on defects larger than 11 nm. To evaluate the defect detection extendibility of the developing PEM optics, defect detection sensitivity of smaller than 16 nm sized defects in hp 64 nm on the mask was evaluated. Hp 64 nm L/S pattern was fabricated by a set of absorber layers that consisted of 14-nm-thick TaBO and 52-nm-thick TaBN on 2.5-nm-thick Ru-cap, on 40 pairs of EUV reflective multi-layers (ML). After enhancing the defect, the pattern signal “without-defect” was subtracted from the signal of “with-defect”. In order to precisely correct the relative displacement between these pattern signals, higher image contrast of mask pattern would be necessary. By a continuous 2D pattern matching, the alignment error is reduced down to be negligibly small. Then, the differential signal higher than the threshold value is identified as the defect signal.

Next, defect detection algorithm adjustment was executed for defect detection sensitivity improvement. The evaluation type of defect was an extrusion defect. Figure 3 shows the defect detection sensitivity evaluation result. The upper row shows SEM image with programmed defects of size 13 nm. The lower row shows the defect detection result with the binary image of image difference and superimposed inspection image. The targeted defect that is marked in a dotted circle is clearly identified although several false defects are also encountered. There is still a need for further improvement to detect the targeted defect without encountering false defects.

Figure 4 shows the defect detection sensitivity evaluation of the intrusion defects. A captured image of a 12-nm intrusion defect in hp 64 nm L/S pattern was used for detection. The upper row shows the SEM image with a programmed defect of size 12 nm. The lower row shows the defect detection result with the binary image of image difference and superimposed inspection image. Applying the image-processing algorithm improvement, the targeted defect marked in the dotted circle is clearly identified without false defects. In order to examine the defect detection sensitivity, which is achieved by the processing image of “without-defect” subtracted from the processing image of “with-defect”, the relationship between signal intensity and defect size was measured for several sizes of programmed defects.

Figure 5 shows the relationship between the defect size and signal intensity. The sensitivity of defect detection is expressed as a defect signal-to-noise ratio.[13] Signal intensity is the defect detection signal at the pixel of the designed defect position. The evaluation types of defects were intrusion and extrusion defects. As the defect size shrinks, signal intensity decreases linearly and is predicted to become zero at the defect size of zero. For the different types of defects, there are similar tendencies between the defect sizes and signal intensities. To realize a higher defect detection sensitivity, signal intensity enhancement by signal processing, image correction by error minimization, error reduction in mask pattern fabrication, and improvement of PEM optics are called for. Comparing the 12 nm sized intrusion defect and 13 nm extrusion defects, the signal intensity of the 12 nm intrusion defect is larger than that of the 13 nm sized extrusion defect. On the condition that the signal deviation of a defect surrounding area remains constant, larger signal intensity can suppress the false defect generation. On the other hand, signal deviation level reduction can reduce the false defect generation while the signal intensity remaining the same. Now we focus on the defect detection signal map generated after enhancing the defect signal. They were run through an image-processing system where the

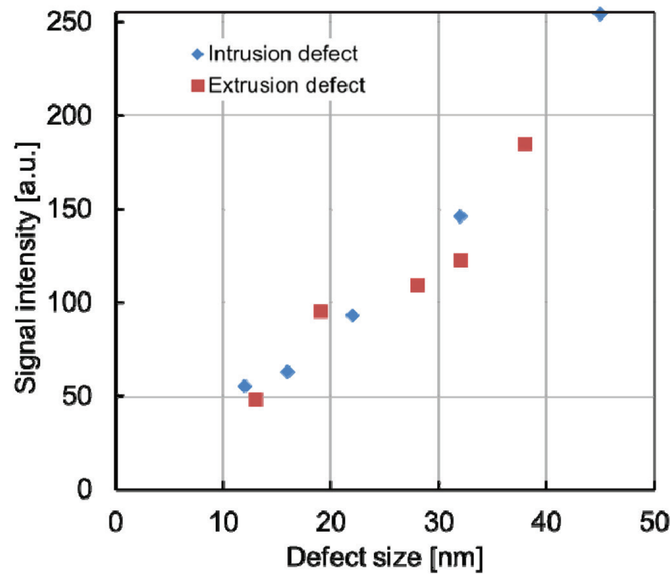

Figure 5. Defect detection sensitivity evaluation result for extrusion defects.

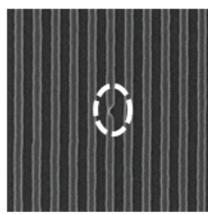

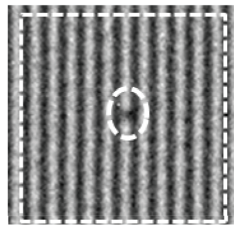

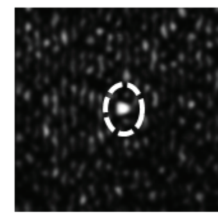

(a) Defect SEM image (b) Captured PEM image (c) Defect detection signal

Figure 6. Defect detection sensitivity evaluation result for extrusion defects.

pattern signal "without-defect" was subtracted from the pattern signal of "with-defect". Figure 6 (a) shows the SEM image of the programmed defect, and (b) shows the PEM image of the actual defect. Figure 6 (c) shows the defect detection signal map. The defect is a 45 nm sized intrusion defect. The programmed defect is arranged in accordance with the center of the area. The targeted defect position is marked in the dotted circle. The signal intensity increases at the position of the defect, and if the signal intensity value exceeds a threshold level set for the defect detection of the targeted defect size, the defect is then identified. On the condition that as the image noise increases, the position where the image signal exceeds the threshold level appears as a defect, which in the actuality is a false defect.

3.2 Defect detection signal intensity distribution analysis for sensitivity improvement

Next, figure 7 (a) shows the picture of a detection signal of a 32 nm size intrusion defect. Fig. 7 (b) shows a histogram of the distribution of the defect detection signal intensity. There are several error causes for defect detection in the image of "with-defect" and "without-defect". So, the generated defect detection signal which was calculated from the processed PEM images has a signal value distribution. While the signal intensity increases, the signal intensity frequency also gradually increases and reaches to a local maximum. Then after that the signal intensity frequency reduces to zero. The histogram of Fig. 7 (b) shows the signal intensity of the targeted defect defined by the position of the target on the x-axis representing signal intensity; and it shows a maximum value of the frequency shown by the peak (4) on the signal intensity distribution not being a representation of the targeted defect. Moving further right on the x-axis, toward the increasing end of the signal intensity scale, a small peak (3) is the representation of a targeted defect with a highest intensity in the region and without the occurrence of false defect. A vertical dotted line defines a border on signal intensity scale (x-axis) that separates the signal intensity distribution region on the map from any information on the targeted defect. On the left-hand side of the border, which is pointed out by an arrow (2), there are all signal intensity distributions except any information related to the targeted defect detection signal in the map. The right-hand side of the border which is pointed out by an arrow (1), there appears only the frequency related to the targeted defect signal intensity. From this relationship, it becomes necessary to achieve sufficient defect signal intensity compared to the signal that may appear from any other position in the map, or to achieve a sufficient difference between the frequencies of

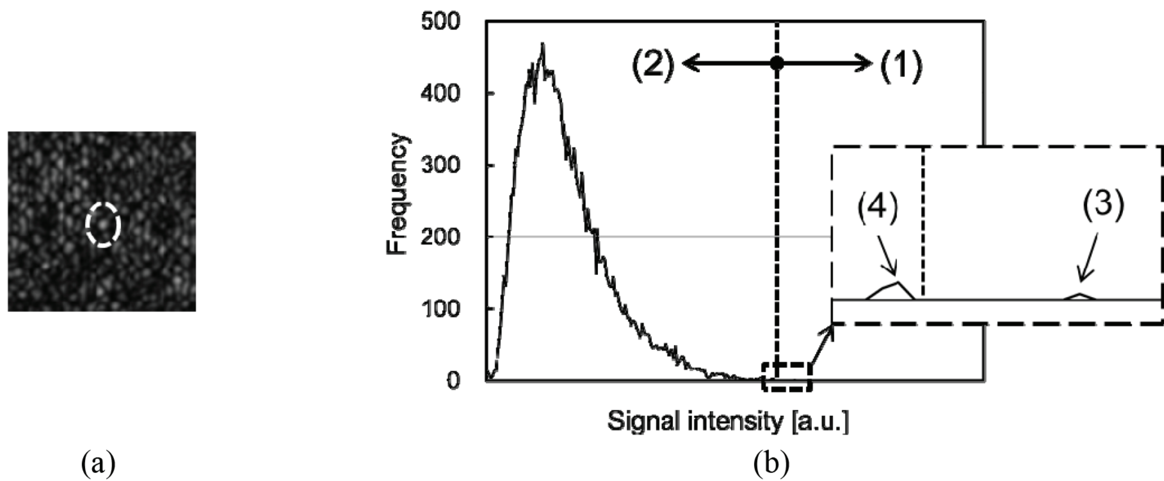

Figure 7. (a) Picture of a detection signal of a 32 nm intrusion defect, (b) Signal intensity distribution map. (1) is the region where there appears only the frequency related to the targeted defect signal intensity. (2) is the region where there appears all signal intensity distributions except any information related to the targeted defect detection signal in the map. (3) is the signal intensity of the targeted defect, (4) shows the maximum value of the signal intensity distribution except for the targeted defect.

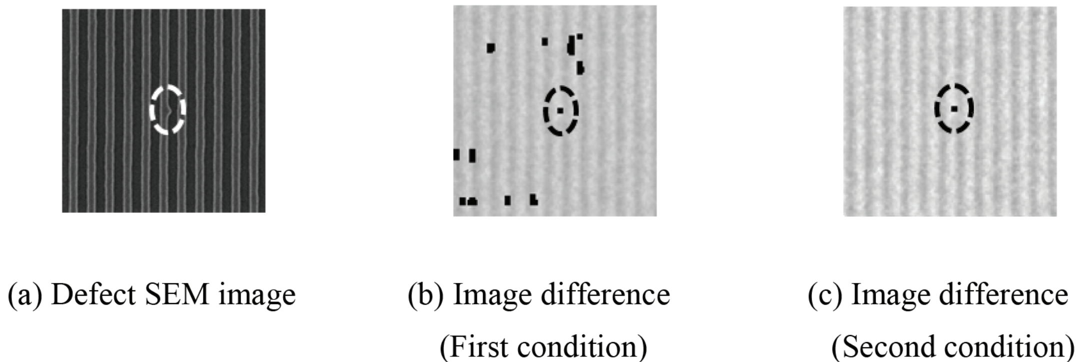

Figure 8. Defect detection results on different conditions.

the signal intensity value and the rest of the intensity values. This is indicated by the dotted line serving as a line of demarcation between the areas (1) and (2) resulting in the formation of the targeted defect signals for detecting the targeted defect without encountering false defects.

Here we think about the conditions that focus on the intensity distribution of the defect detection map without false defects. It was found from the signal intensity distribution with small image-noise (except for the targeted defect) that the characteristics of the images "with-defect" and "without defect" were very much the same. But, image acquisition procedure has as many error factors that generate the image characteristics' deviations. Intra-field image intensity deviation causes intensity fluctuation of the defect detection signal, which leads to the generation of false defects. And, to execute a full area of mask inspection, the mask is scanned in Y direction where a swath image of mask pattern is captured using the TDI mode, and then stepped in X direction. By repeating the step and scan movement, full mask area is thus inspected. The mask position measurement deviation leads to the image position error in calculating the subtracted image of "without-defect" from the processing image of "with-defect". This error generates a signal difference which is recognized as the false defects. So, the image characteristics' adjustment, such as comparing the image profile of L/S pattern between the image of "with-defect" and "without-defect", was executed in order to align the position of each image precisely. The deviation of L/S pattern profile contrast or the signal offset fluctuation caused by the illumination intensity unevenness produces the alignment error. To realize a high-precision alignment between the image of "without-defect" and the image of "with-defect", it is important to adjust the image characteristics such as illumination unevenness or deviation of L/S pattern profile contrast in advance. Image adjustment effect of the captured images of "with-defect" and "without-defect" was evaluated before the defect detection image-processing sequence. Defect detection sensitivity evaluations are executed under two different conditions as described in below:

First, captured raw images of "with-defect" and "without-defect" are applied for defect detection image-processing. Second, intra-field illumination unevenness and L/S pattern image contrast deviation adjustments are performed in advance, before the defect detection sequence is executed. Figure 8 shows the defect detection results of these two conditions. The defect detection signal

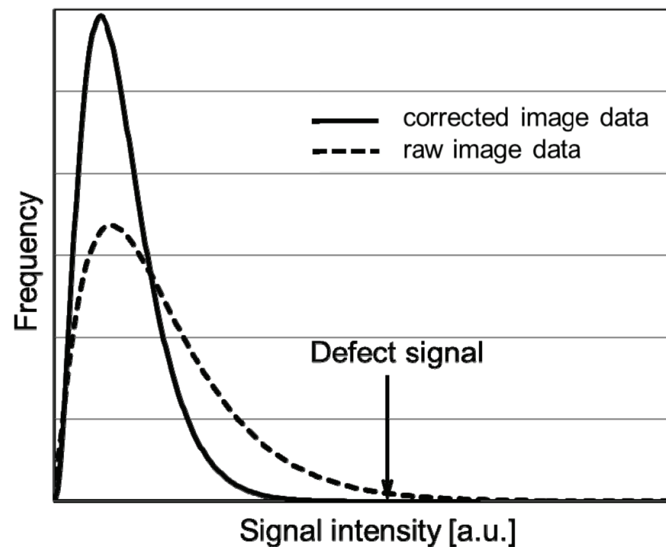

Figure 9. Fitted probability density function curves from the raw image data and adjusted image data.

threshold was normalized by the defect detection signal of the targeted defect. Figure 8(a) shows the SEM image of programmed defect, and Figs. (b) and (c) show the binary images of the image difference and superimposed inspection images on the conditions of the first and second cases. Targeted defect was identified as the center of the dotted circle, although several false defects were also detected as shown in Fig. 8 (b).

By applying the image adjustment to the captured images, the targeted defects that are marked in the dotted circles are clearly identified without false defects as shown in Fig. 8 (c). For these two conditions, signal intensity distribution is compared to examine the effect of image adjustment. Signal intensity histograms were fitted by the gamma distribution as the probability density function. Fitted results show good agreements with signal intensity distribution from the raw image data and adjusted image data. Figure 9 shows the fitted probability density function curves from the raw image data and corrected image data. Comparing these two curves, the image adjustment increases the signal difference between the defect signal intensity and the maximum signal intensity that does not include that of the targeted defect in the defect detection signal map. From these results, it is confirmed that the signal intensity distribution change has its influence on the false defect generation in defect detection sequence. To suppress the generation of false defect and to realize the high sensitivity defect detection, investigation of the signal intensity distribution, and signal adjustment that can reduce the maximum value of the signal intensity distribution except the targeted defect, would be required.

4. Summary and Conclusion

We have selected our PEM system for inspection optics because of its good performance for 16 nm node EUV mask pattern inspection and its capability for detecting several types of defects. Now we continue to investigate for the refinement of the 16 nm generation inspection performance down to 11 nm. In addition to the 16 nm intrusion programmed defect in hp 64 nm on the mask, which was clearly observed by applying the image-processing algorithm improvement, defect detection sensitivity of smaller than 16 nm sized defects in hp 64 nm on the mask could be evaluated. As the defect size shrinks, signal intensity decreases; and the linear relationship between the defect size and signal intensity is thus investigated. 13 nm sized extrusion defect is clearly identified although several false defects are also detected. Applying the image-processing algorithm improvement, the 12 nm sized intrusion defect is clearly identified without encountering false defects. It is confirmed that the developing PEM optics has the potential for sub-16 nm node mask pattern inspection. The defect detection condition for a higher defect inspection sensitivity without false defect was discussed. While the signal intensity increases, signal intensity frequency increases gradually and reaches to a local maximum. Then the signal intensity frequency reduces to zero. So the signal intensity of the targeted defect size is larger than at the position where the signal intensity frequency was less than 1. Signal intensity histograms were fitted by the gamma distribution as the probability density function; and the fitted results have good agreement with the experiments. Image adjustment effect of the captured images of “with-defect” and “without-defect” was evaluated before the start of the defect detection image-processing sequence. Image correction of intra-field illumination unevenness and L/S pattern image contrast deviation suppress the generation of the false defects. It is confirmed that the signal intensity distribution change has the influence in the false defect generation of defect detection sequence. As the next step, development for the defect detection signal enhancement and false defect reduction technique by mitigating the captured image error will be addressed for the refinement of 16 nm generation inspection performance down to 11nm.

5. Acknowledgement

The authors would like to thank the following people from Toshiba Corporation: Masato Naka, Ryoji Yoshikawa, Takashi Hirano, and Masamitsu Itoh; the following people from EBARA CORPORATION: Tsutomu Karimata, Kenji Watanabe, Ryo Tajima and Yasushi Tohma for their technical support, and NANOTECH CO., LTD. for their designing and installation of electronics for the developing

PEM system, as well as Ms. W. Asada of EUVL Infrastructure Development Center, Inc. (EIDEC) for analyzing the data. This work is supported by New Energy and Industrial Technology Development Organization (NEDO) and Ministry of Economy, Trade and Industry (METI).

7. References

[1] R. Hirano, N. Kikuiri, H. Hashimoto, K. Takahara, M. Hirono, and H. Shigemura, "Study of EUV mask inspection technique using DUV light source for hp22nm and beyond", **Proc. SPIE 7823**, 782339 (2010).

[2] S. Yamaguchi, M. Naka, M. Kadowaki, T. Koike, T. Hirano, M. Itoh, Y. Yamazaki, K. Terao, M. Hatakeyama, K. Watanabe, H. Sobukawa, T. Murakami, K. Tsukamoto, T. Hayashi, N. Kimura, and N. Hayashi, "Performance of EBeyeM for EUV Mask Inspection", **Proc. SPIE 8166**, 81662F (2011).

[3] T. Shimomura, S. Kawashima, Y. Inazuki, T. Abe, T. Takikawa, H. Mohri, N. Hayashi, F. Wang, L. Ma, Y. Zhao, C. Kuan, H. Xiao, and J. Jau, "Demonstration of defect free EUV mask for 22 nm NAND flash contact Layer using electron beam inspection system", **Proc. SPIE 7969**, 79691B (2011).

[4] T. Hirano, S. Yamaguchi, M. Naka, M. Itoh, M. Kadowaki, T. Koike, Y. Yamazaki, K. Terao, M. Hatakeyama, H. Sobukawa, T. Murakami, K. Tsukamoto, T. Hayashi, K. Watanabe, N. Kimura, and N. Hayashi, "Development of EB inspection system EBeyeM for EUV mask", **Proc. SPIE 7823**, 78232C (2010).

[5] R. Hirano, H. Watanabe, S. Iida, T. Amano, T. Terasawa, M. Hatakeyama, and T. Murakami, "Study of EUV mask inspection using projection EB optics with programmed pattern defect", **Proc. SPIE 8441**, 84411G-1 (2012).

[6] International Technology Roadmap for Semiconductors 2012 Update, Lithography, Table LITH6

[7] M. Miyoshi, Y. Yamazaki, I. Nagahama, A. Onishi, and K. Okumura, "Electron beam inspection system based on the projection imaging electron microscope", *J. Vac. Sci. Technol.* **B19 (6)**, pp.2852-2855 (2001).

[8] T. Amano, S. Iida, R. Hirano, T. Terasawa, H. Watanabe, M. Hatakeyama, and T. Murakami, "EUV mask pattern inspection using EB projection optics" 2011 Inter. Symposium on EUVL, 17-19 October Miami, US (2011).

[9] R. Hirano, H. Watanabe, S Iida, T. Amano, T. Terasawa, M. Hatakeyama, and T. Murakami, "Development of extreme ultraviolet mask pattern inspection technology using projection electron beam optics", *J. Micro/Nanolith. MEMS MOEMS* **12(2)**, 021003 (2013). Proc. of SPIE Vol. 9235 92351C-10

[10] R. Hirano, S Iida, T. Amano, T. Terasawa, H. Watanabe, M. Hatakeyama, T. Murakami, and K. Terao, "Patterned mask inspection technology with projection electron microscope technique on extreme ultraviolet masks", *J. Micro/Nanolith. MEMS MOEMS* **13**, 013009 (2014).

[11] H. Watanabe, R. Hirano, S. Iida, T. Amano, T. Terasawa, M. Hatakeyama, T. Murakami, S. Yoshikawa, and K. Terao, "EUV patterned mask inspection system using a projection electron microscope technique", **Proc. SPIE 8880**, 88800U (2013).

[12] M. Hatakeyama, T. Murakami, K. Terao, K. Watanabe, S. Yoshikawa, T. Amano, R. Hirano, S. Iida, T. Terasawa, and H. Watanabe, " Development of Inspection System for EUV Mask with Novel Projection Electron Microscopy (PEM)", **Proc. SPIE 8880**, 888028 (2013).

[13] R. Hirano, S. Iida, T. Amano, T. Terasawa, H. Watanabe, M. Hatakeyama, T. Murakami, and K. Terao, "EUV patterned mask inspection with an advanced Projection Electron Microscope (PEM) system", **Proc. SPIE 9048**, 90480Z-1 (2014).

[14] International Technology Roadmap for Semiconductors 2013 Edition, Lithography, Table LITH6

[15] T. Terasawa, Y. Arisawa, T. Amano, T. Yamane, H. Watanabe, M. Toyoda, T. Harada, and H. Kinoshita, "Simulation Analysis of the Characteristics of a High Magnification Imaging Optics for the Observation of Extreme Ultraviolet Lithography Mask to Predict Phase Defect Printability", *Jpn. J. Appl. Phys.* **52** 096601 (2013).

[16] R. Hirano, S. Iida, T. Amano, T. Terasawa, H. Watanabe, M. Hatakeyama, T. Murakami, and K. Terao, "EUV patterned mask inspection performance of an advanced projection electron microscope (PEM) system for hp 16 nm and beyond", **Proc. SPIE 9256**, 92560M-4 (2014).

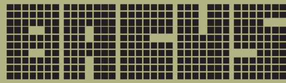

N • E • W • S

Sponsorship Opportunities

Sign up now for the best sponsorship opportunities

Photomask 2015 —
Contact: Lara Miles, Tel: +1 360 676 3290; laram@spie.org

Advanced Lithography 2016 —
Contact: Lara Miles, Tel: +1 360 676 3290; laram@spie.org

Advertise in the BACUS News!

The BACUS Newsletter is the premier publication serving the photomask industry. For information on how to advertise, contact:

Lara Miles
Tel: +1 360 676 3290
laram@spie.org

BACUS Corporate Members

Acuphase Inc.
American Coating Technologies LLC
AMETEK Precitech, Inc.
Berliner Glas KGaA Herbert Kubatz GmbH & Co.
FUJIFILM Electronic Materials U.S.A., Inc.
Gudeng Precision Industrial Co., Ltd.
Halocarbon Products
HamaTech APE GmbH & Co. KG
Hitachi High Technologies America, Inc.
JEOL USA Inc.
Mentor Graphics Corp.
Molecular Imprints, Inc.
Panavision Federal Systems, LLC
Profilocolore Srl
Raytheon ELCAN Optical Technologies
XYALIS

Industry Briefs

SEMI Reports 2014 Semiconductor Photomask Sales of $3.2B

By: **Solid State Technology**

SEMI reports that the worldwide semiconductor photomask market was $3.2 billion in 2014 and is forecasted to reach $3.4 billion in 2016. After increasing 1 percent in 2013, it increased 3 percent in 2014 and is expected to grow 4 and 3 percent in 2015 and 2016, respectively. Key drivers continue to be advanced feature sizes (less than 45 nm) and increased manufacturing in Asia-Pacific. Taiwan remains the largest regional market for the fifth year in a row and is expected to be largest for the duration of the forecast.

Revenues of $3.2 billion place photomasks at 13 percent of the total wafer fabrication materials market, behind silicon and semiconductor gases. By comparison, photomasks represented 18 percent of the total wafer fabrication materials in 2003. Another trend is the increasing importance of captive mask shops. Captive mask shops, aided by intense capital expenditures in 2011 and 2012 and a weakening Yen in 2013 and 2014, gained market share at merchant suppliers' expense, accounting for 53 percent of the total photomask market last year, up from 49 percent in 2013. They represented 31 percent of the photomask market in 2003. A recent published SEMI report, "2014 Photomask Characterization Summary," provides details, includes data from 2003 to 2016, and summarizes lithography developments over the past year.

Moore's Law Hits Middle Age Tales from Engineers Who Drove it Forward

By: **Rick Merritt,** EETIMES

SAN JOSE, Calif. — On April 19, 1965, Electronics magazine published a paper in which Gordon Moore made a stunning observation: About every two years, engineers should be able to cram twice as many transistors into the same area of a silicon chip. Over the next 50 years, engineers more or less managed to maintain that predicted pace of innovation, delivering dramatically better semiconductors. Their efforts were central to the seeming magic of a high tech sector riding an exponential growth curve that became known as Moore's law. Of the thousands of engineers who have kept Moore's law going, EE Times interviewed top chip technologists who shared their stories and optimism that progress will continue.

To date the progress Moore's law represents has not been limited to "just ever faster and cheaper computers but an infinite number of new applications from communications and the Internet to smart phones and tablets," said Robert Maire, a semiconductor analysts in a recent newsletter. The benefits are measured in trillions of dollars, according to G. Dan Hutcheson, chief executive of VLSI Research. He calculates the deflationary value of packing more features into the same silicon area at $67.8 billion last year alone, with a knock-on value of half a trillion dollars to the overall electronics industry that used the chips. "The market value of the companies across the spectrum of technology driven by Moore's Law amounted to $13 trillion in 2014," Hutchison estimated. "Another way to put it is that one-fifth of the asset value in the world's economy would be wiped out if the integrated circuit had not been invented and Moore's law never happened," he said.

Imec Honors Morris Chang

By: **David Manners,** Electronics Weekly

Imec will present its lifetime innovation award to Morris Chang at its June Technology forum in Brussels, for 'profound and unparalleled impact on the global semiconductor industry.'

'By not competing with customers, TSMC enabled entrepreneurs to build world-class businesses around designing and marketing chips without the need of a manufacturing facility,' says Imec, 'by partnering for manufacturing capabilities, fabless companies can avoid the mammoth costs of operating their own semiconductor fabrication facility and focus on innovation of the circuits.' (…) "Chairman Chang is immensely respected in the global semiconductor community for his innovative vision and tireless drive to shape the future of technology," says Imec CEO Luc Van den hove. Since 2005, TSMC has been one of the core partners in Imec's industrial affiliation program on advanced CMOS technologies. Imec's unique research platform harnesses the collective expertise and knowledge of the entire value chain of foundries, IDMs, fabless and fab-lite companies, packaging and assembly companies, and equipment and material suppliers.

Join the premier professional organization for mask makers and mask users!

About the BACUS Group

Founded in 1980 by a group of chrome blank users wanting a single voice to interact with suppliers, BACUS has grown to become the largest and most widely known forum for the exchange of technical information of interest to photomask and reticle makers. BACUS joined SPIE in January of 1991 to expand the exchange of information with mask makers around the world.

The group sponsors an informative monthly meeting and newsletter, BACUS News. The BACUS annual Photomask Technology Symposium covers photomask technology, photomask processes, lithography, materials and resists, phase shift masks, inspection and repair, metrology, and quality and manufacturing management.

Individual Membership Benefits include:

- Subscription to BACUS News (monthly)
- Eligibility to hold office on BACUS Steering Committee

www.spie.org/bacushome

Corporate Membership Benefits include:

- 3-10 Voting Members in the SPIE General Membership, depending on tier level
- Subscription to BACUS News (monthly)
- One online SPIE Journal Subscription
- Listed as a Corporate Member in the BACUS Monthly Newsletter

www.spie.org/bacushome

Calendar

2015

SPIE Photomask Technology
29 September-1 October 2015
Monterey Marriott and
Monterey Conference Center
Monterey, California, USA
www.spie.org/pm

Co-located with
SPIE Scanning Microscopies
www.spie.org/sg

2016

SPIE Advanced Lithography
San Jose Convention Center
and San Jose Marriott
San Jose, California, USA
www.spie.org/al

SPIE Advanced Lithography call will be available late April 2015.

SPIE is the international society for optics and photonics, a not-for-profit organization founded in 1955 to advance light-based technologies. The Society serves nearly 225,000 constituents from approximately 150 countries, offering conferences, continuing education, books, journals, and a digital library in support of interdisciplinary information exchange, professional growth, and patent precedent. SPIE provided over $3.4 million in support of education and outreach programs in 2014.

SPIE.
International Headquarters
P.O. Box 10, Bellingham, WA 98227-0010 USA
Tel: +1 360 676 3290
Fax: +1 360 647 1445
help@spie.org • www.SPIE.org

Shipping Address
1000 20th St., Bellingham, WA 98225-6705 USA

Managed by SPIE Europe
2 Alexandra Gate, Ffordd Pengam, Cardiff,
CF24 2SA, UK
Tel: +44 29 2089 4747
Fax: +44 29 2089 4750
spieeurope@spieeurope.org • www.spieeurope.org

You are invited to submit events of interest for this calendar. Please send to lindad@spie.org; alternatively, email or fax to SPIE.